26th ABCM International Congress of Mechanical Engineering
November 22-26, 2021. Florianópolis, SC, Brazil

COB-2021-1760
CONTINUUM STRONG DISCONTINUITY APPROACH IN THE CONTEXT OF BOUNDARY ELEMENT METHOD FOR STRUCTURAL ANALYSIS OF THREE-DIMENSIONAL BRITTLE SOLIDS

Alisson Pinto Chaves
Rodrigo Guerra Peixoto
Ramon Pereira da Silva
Universidade Federal de Minas Gerais, Departamento de Engenharia de Estruturas, Av. Antônio Carlos 6627, Belo Horizonte, Minas Gerais, Brazil
alissonpchaves@ufmg.br; rodrigo.peixoto@dees.ufmg.br; ramon@ufmg.br

Abstract. *Since its introduction, the Continuum Strong Discontinuity Approach (CSDA) has been widely used with the Finite Element Method (FEM), and its efficiency and accuracy is demonstrated in a series of works. In this approach, a set of kinematic equations (regularized formulation) is used to describe displacements and strains at a discontinuity surface. It uses an intrinsic softening parameter, as a re-interpretation of softening modulus from continuum constitutive model. The jump displacement components are evaluated with additional equations, obtained by the assumption of continuity condition of the traction vector on the discontinuity surface. Thus, applying this regularized kinematic on ordinary continuous constitutive models, the consistent discrete model obtained can relate traction with displacement jumps where the discontinuity is established. This work presents some first steps in the use of the Implicit Boundary Element Method (BEM) associated with the CSDA for the modeling of crack growth in physically non-linear three-dimensional problems of solid mechanics. This non-geometrical approach has been successfully used in the analysis of plane problems. An isotropic damage constitutive model is used to represent damage dissipation in finite regions of a solid domain, over the discontinuity surface. In this work, the strong discontinuity regime is imposed directly after the end of the elastic regime with the discontinuity plane defined as perpendicular to the maximum principal stress. Quadrilateral isotropic boundary elements are used together with hexahedral constant cells with embedded discontinuity. Only the region of the domain where the crack surface is supposed to be located need to be discretized, while the remaining non-discretized regions are considered to work in elastic regime. The implementations were performed on the collaborative open source system INSANE. A numerical example illustrates the performance of the approach and particularities.*

Keywords: *Continuum Strong Discontinuity Approach, Implicit Boundary Element Method, Three-dimensional Modeling, Non-linear Analysis*

1. INTRODUCTION

The continuum strong discontinuity approach (CSDA), was firstly introduced by Simo *et al.* (1993). This approach uses a set of kinematic equations, in a regularized formulation, to describe displacements and strains at a discontinuity surface (Oliver *et al.*, 1998). An intrinsic softening modulus, which is obtained as a material parameter from an energy dissipation analysis in the fracture process, is used as a re-interpretation of the softening modulus from a continuum constitutive model. The jump displacement components are evaluated with additional equations, obtained by the assumption of continuity condition of the traction vector on the discontinuity surface. Thus, applying this regularized kinematic on ordinary continuous constitutive models, the consistent discrete model obtained can relate traction with displacement jumps where the discontinuity is established.

The CSDA is appropriate to describe macroscopic cracks, but can also be used to represent precedent micro-cracks that arises during its formation in some materials. For those materials (quasi-brittle), this transitional phase from smeared to macroscopic crack correspond to a weak discontinuity regime, in which the strain field is discontinuous whereas the displacement field remains continuous, forming a strain localization band. Once the strong discontinuity regime takes place, the displacement field turns discontinuous whereas the strain field became unbounded. The CSDA formulation can be used for the cases of weak or strong discontinuities. The second one can be understood as a special case of the first with the bandwidth tending to zero.

Since its introduction, the CSDA has become an important branch of the non-geometric approach to the analysis of crack development by computational fracture mechanics (CFM). Its use, associated with the FEM, had the efficiency

and accuracy demonstrated in a series of works, *e.g.* Oliver *et al.* (1999, 2002, 2003), and also with the generalized (or extended) finite element method (G/X-FEM) (Mariani and Perego, 2003; Oliver *et al.*, 2006b). The use of CSDA in the context of the boundary element method (BEM) was firstly proposed by Manzoli and Venturini (2004, 2007).

The boundary element method has been used for the structural analyses of solids with physically non-linear behavior since its origins when it was still known as boundary integral equation method. Telles and Carrer (1991) proposed an implicit formulation using the proportional relationship between rates of stress and elastic strain, based on the previous work of Telles and Brebbia (1979). The initial field increments were written in terms of total strain, resulting in a discrete equilibrium equation, which is linearized and incrementally solved. This formulation works accordingly for elastoplastic constitutive models, nevertheless Lin *et al.* (2002); Sládek *et al.* (2003); Botta *et al.* (2005); Benallal *et al.* (2006) related some problems when dealing with quasi-brittle materials, like mesh dependence associated with strain localization and the need for non-local strategy for regularization. Peixoto *et al.* (2017) shown the CSDA as a limit case of strain localization in the implicit BEM formulation. Therefore, the use of CSDA seems suitable, as the standard continuum constitutive model can be applied even for unlimited strains that are compatible with discontinuous displacement field.

Using implicit BEM, Manzoli and Venturini (2004, 2007) introduced discontinuity interfaces inside triangular cells that discretized the whole domain. They used associative elastoplastic constitutive models with a specific yield criterion, together with an exponential softening law to represent the behaviour of crack in quasi-brittle materials. Later, this idea was extended by using an isotropic damage model and a tracking algorithm to generate cells automatically, in the direction of the crack path determined during the analyses (Manzoli *et al.*, 2009). A further improvement was presented by Peixoto *et al.* (2017, 2018), who sophisticated the non-linear analysis, involving inelastic dissipation with softening in continuous media, bifurcation analysis and transition between weak and strong discontinuities. They used subparametric quadrilateral cells with constant approach (uniform displacement jumps) with another automatic cells generation algorithm. They also reported some stress locking phenomena, also observed in FEM-CSDA (Oliver *et al.*, 2003), which has been overcome by using non-uniform displacement jumps inside the cells, as proposed by (Mendonça *et al.*, 2020).

The use of CSDA in the context of BEM is, so far, limited to two-dimensional problems. This work presents some first steps for the extension of this methodology to three-dimensional problems. An elastic-degrading constitutive model with an exponential softening law for isotropic materials is considered together with the CSDA. The strong discontinuity regime is imposed directly after the end of the elastic regime with the discontinuity surface defined as perpendicular to the maximum principal stress. This is understood as a typical behaviour of isotropic brittle materials. Quadrilateral linear isoparametric boundary elements are used together with hexahedral constant cells with embedded discontinuity. Those cells were placed aligned along the previously known crack surface. The implementations were performed based on the previous development reported in Anacleto *et al.* (2013) and Peixoto *et al.* (2016) at the collaborative open source system INSANE (INteractive Structural ANalysis Environment).

2. STRONG DISCONTINUITY APPROACH

Incorporation of strong discontinuity approach in the standard integral equations requires some adaptation, resulting in equations summarized in this section.

2.1 Kinematic of Strong Discontinuity

Consider the solid represented in Fig. 1 (domain Ω, boundary Γ), with a discontinuity surface $\mathcal{S}$ (unitary normal vector $\mathbf{n}$), surrounded by an arbitrary sub-domain $\Omega_\varphi \subset \Omega$.

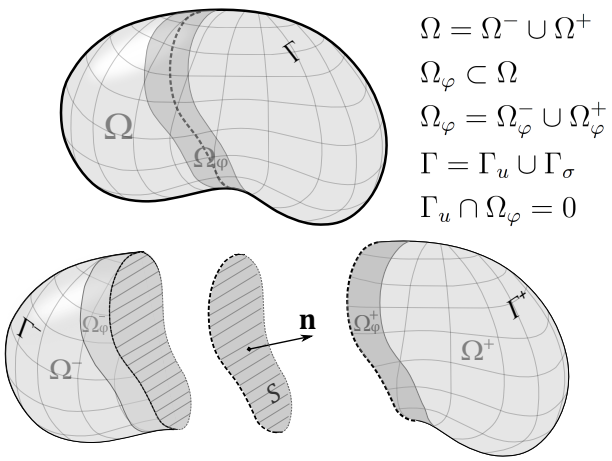

Figure 1: Solid with discontinuity surface $\mathcal{S}$ in an arbitrary sub-domain Ω_φ

For a material point $\mathbf{X}$, an arbitrary function $\varphi(\mathbf{X})$ is defined in Ω_φ, and the conditions outside Ω_φ are shown in Fig. 2. Together with the well known Heaviside function ($\mathcal{H}$), at a given instant when the strong discontinuity is completely developed, the displacement and the total strain field can be described by the regularized expression detailed in Peixoto *et al.* (2017, 2018) as follows:

$$u_i(\mathbf{X},t) = \underbrace{\bar{u}_i(\mathbf{X},t) + \varphi(\mathbf{X})[\![u_i]\!](\mathbf{X},t)}_{\hat{u}_i(\mathbf{X},t)} + \underbrace{\big[\mathcal{H}_\mathcal{S}(\mathbf{X}) - \varphi(\mathbf{X})\big]}_{\mathcal{M}^\varphi_\mathcal{S}(\mathbf{X})}[\![u_i]\!](\mathbf{X},t) = \hat{u}_i(\mathbf{X},t) + \mathcal{M}^\varphi_\mathcal{S}(\mathbf{X})[\![u_i]\!](\mathbf{X},t) \tag{1}$$

$$\epsilon_{ij}(\mathbf{X},t) = \underbrace{\frac{1}{2}(\hat{u}_{i,j} + \hat{u}_{j,i})}_{\hat{\epsilon}_{ij}} + \underbrace{\frac{\mathcal{M}^\varphi_\mathcal{S}}{2}([\![u_{i,j}]\!] + [\![u_{j,i}]\!]) - \frac{1}{2}(\varphi_{,i}[\![u_j]\!] + \varphi_{,j}[\![u_i]\!])}_{-\epsilon^\varphi_{ij}} + \frac{\delta_\mathcal{S}}{2}\big([\![u_i]\!]n_j + [\![u_j]\!]n_i\big) \tag{2}$$

where $\bar{u}_i(\mathbf{X},t)$ is the regular part of the displacement field, $[\![u_i]\!](\mathbf{X},t)$ is the displacement jump component on the discontinuity surface, and $\hat{u}_i(\mathbf{X},t)$ represents a continuous function. Complementing, $\mathcal{M}^\varphi_\mathcal{S}(\mathbf{X})$ takes zero value everywhere in Ω, except in Ω_φ, as shown in Fig. 2. Also, $\hat{\epsilon}_{ij}$ is the regular term and ϵ^φ_{ij} has null value outside the sub-domain Ω_φ. Finally, the last term in Eq. 2 is restricted to the discontinuity surface, where n_j are components of its unitary normal vector, and $\delta_\mathcal{S}$ represents the Dirac delta function over $\mathcal{S}$.

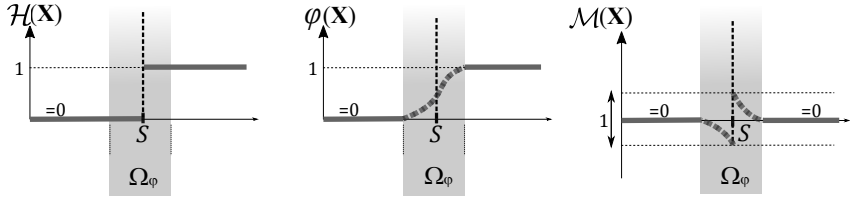

Figure 2: Functions: $\mathcal{H}_\mathcal{S}(\mathbf{X})$, $\varphi(\mathbf{X})$, and $\mathcal{M}^\varphi_\mathcal{S}$

2.2 Constitutive and equilibrium equations for the discontinuity interface

Once the discontinuity exists, it is necessary to contemplate some conditions that make the discontinuous kinematic compatible with a constitutive model, through the expression of traction-displacement relationship, instead of the usual stress-strain. At the discontinuity interface, the equilibrium condition requires the continuity of the traction vector, i.e. $\sigma^{\Omega\setminus\mathcal{S}}_{ij} n_j = \sigma^\mathcal{S}_{ij} n_j$, as well as its rates ($\sigma^\mathcal{S}_{ij}$ represent stress components on $\mathcal{S}$, while $\sigma^{\Omega\setminus\mathcal{S}}_{ij}$ represent stress components at other domain points, particularly, in an infinitesimally close point to $\mathcal{S}$). Thus, for this condition, at an instant of time, the following equation must be satisfied for points at the discontinuity surface:

$$f_i(\hat{\epsilon}_{ij}, [\![u_i]\!], [\![u_{i,j}]\!]) = \big[\sigma^{\Omega\setminus\mathcal{S}}_{ij}(\epsilon_{ij}) - \sigma^\mathcal{S}_{ij}(\epsilon_{ij})\big]n_j = \big\{E^o_{ijkl}\big[\hat{\epsilon}_{kl} - \epsilon^\varphi_{kl}([\![u_i]\!], [\![u_{i,j}]\!])\big] - \sigma^\mathcal{S}_{ij}(\epsilon_{ij})\big\}n_j = 0 \tag{3}$$

For the BEM formulation used in this work, the domain is discretized only where the discontinuity settles down, by using cells with embedded discontinuity. Inside each cell, the components ϵ^φ_{ij} are functions of the displacement jump components, $[\![u_i]\!]$ only, once they can be assumed to be constant inside each cell ($[\![u_{i,j}]\!] = 0$). Thus, for a given regular strain $\hat{\epsilon}_{ij}$, the only unknown variables from Eq. (3) are the components $[\![u_i]\!]$, i.e. $f_i \equiv f_i([\![u_i]\!]) = 0$. These components can be evaluated iteratively through the linearisation of Eq. (3). Then, for a given $[\![u_i]\!](\hat{\epsilon}_{ij})$ achieved from the solution of Eq. (3), a constitutive regularized equation can be obtained, as follows:

$$\tilde{\sigma}_{ij}(\hat{\epsilon}_{ij}) = \sigma^{\Omega\setminus\mathcal{S}}_{ij}\big(\hat{\epsilon}_{ij} - \epsilon^\varphi_{ij}([\![u_i]\!])\big) = E^o_{ijkl}(\hat{\epsilon}_{kl} - \epsilon^\varphi_{kl}) \tag{4}$$

3. IMPLICIT BEM FORMULATION

For the analysis of solids formed by materials with non-linear behaviour, the BEM have well known equations that can be adapted in order to contemplate the strong discontinuity formulation. The three governing equations: the Somigliana's identity for displacements at internal points, the displacement boundary integral equation and the integral equation for internal strains, can be written with the discontinuity terms.

Once natural and essential boundary conditions are applied at the discretized boundary, those three governing equations can be rearranged in the following discrete equations:

$$\{\dot{\hat{u}}^\Omega\} = [A^u]\{\dot{x}\} + [B^u]\{\dot{y}\} + [Q^u_{\epsilon^\varphi}]\{\dot{\epsilon}^\varphi\} \tag{5}$$

$$[A]\{\dot{x}\} = [B]\{\dot{y}\} + [Q_{\epsilon^\varphi}]\{\dot{\epsilon}^\varphi\} \tag{6}$$

$$\{\dot{\hat{\epsilon}}\} = [A^\epsilon]\{\dot{x}\} + [B^\epsilon]\{\dot{y}\} + [Q^\epsilon_{\epsilon^\varphi}]\{\dot{\epsilon}^\varphi\} \tag{7}$$

where $\{\dot{x}\}$ and $\{\dot{y}\}$ are, respectively, the boundary unknowns and the prescribed values of displacement $\dot{\hat{u}}_i$ or traction $\dot{t}_i$, while $\{\dot{u}^{\Omega}\}$ and $\{\dot{\hat{\epsilon}}\}$ are relative to internal collocation points. The term $\{\dot{\epsilon}^{\varphi}\}$ represents the inelastic strain components and matrices referenced by $[A]$, $[B]$ contain the integrals over the boundary elements, adding the free term c_{ij} where appropriate. Matrices $[Q]$ hold the integrals over internal cells, adding conveniently the free terms $F^{\epsilon\epsilon}_{ijkl}$ in $[Q^{\epsilon}_{\epsilon^{\varphi}}]$.

Following the implicit BEM procedure, Eq. (6) can be solved for $\{\dot{x}\}$ and substituted into Eq. (7), giving:

$$\{\dot{\hat{\epsilon}}\} = [N^{\epsilon}]\{\dot{y}\} + [M^{\epsilon}_{\epsilon^{\varphi}}]\{\dot{\epsilon}^{\varphi}\};\ \text{with:}\ [N^{\epsilon}] = [A^{\epsilon}][A^{-1}][B] + [B^{\epsilon}]\ \text{ and }\ [M^{\epsilon}_{\epsilon^{\varphi}}] = [A^{\epsilon}][A^{-1}][Q_{\epsilon^{\varphi}}] + [Q^{\epsilon}_{\epsilon^{\varphi}}] \tag{8}$$

Regarding the rate independent constitutive damage model considered in this work, time evolution of non-linear analysis can be considered as finite incremental differences, i.e. $(step) = (step)_i - (step)_{i-1}$. Hence, for the *i-th* increment, Eq. (8) turns:

$$\{\hat{\epsilon}\}^i = \lambda^i [N^{\epsilon}]\{y\} + [M^{\epsilon}_{\epsilon^{\varphi}}]\{\epsilon^{\varphi}\}^i \tag{9}$$

where the load factor λ^i is a cumulative scalar value for load increment, defined by the control method employed.

In a given step i, an equilibrium (or residual) vector $\{Q\}^i$ can be defined as a function of the regular strains and the load factor $\{Q(\hat{\epsilon}^i, \lambda^i)\}^i$ as follows:

$$\{Q\}^i = \lambda^i \underbrace{[N^{\epsilon}]\{y\}}_{\{P\}} + \underbrace{[M^{\epsilon}_{\epsilon^{\varphi}}]\big(\{\epsilon\}^i - [E^o]^{-1}\{\tilde{\sigma}(\hat{\epsilon})\}^i\big) - \{\hat{\epsilon}\}^i}_{-\{F\}^i} = \{0\} \tag{10}$$

where $[E^o]$ represents the linear elastic constitutive relationship matrix and $\{\tilde{\sigma}(\hat{\epsilon})\}$ is the stress vector, obtained from the regular strains, as depicted in Eq. (4), the regularized constitutive equation.

The equilibrium condition setted in Eq. (10) has to be verified at each load increment. This can be performed numerically through the Newton's method. A detailed description of this adopted incremental-iterative solution strategy, and the control method employed can be seen in Peixoto *et al.* (2018, 2016).

4. INTERFACE CONSTITUTIVE MODEL

An isotropic damage constitutive model is used in this work to represent damage dissipation in finite regions of a solid domain, over the discontinuity surface. The next expressions synthesize this model:

$$\text{Free energy:}\quad \psi(\epsilon_{ij}, r) = \big[1 - D(r)\big]\psi_o(\epsilon_{ij}),\ \ \psi_o(\epsilon_{ij}) = \frac{1}{2}\epsilon_{ij}E^o_{ijkl}\epsilon_{kl} \tag{11a}$$

$$\text{Constitutive equation:}\quad \sigma^{\mathcal{S}}_{ij} = \frac{\partial\psi(\epsilon_{ij}, r)}{\partial\epsilon_{ij}} = (1-D)E^o_{ijkl}\epsilon_{kl} = E_{ijkl}\epsilon_{kl} \tag{11b}$$

$$\text{Damage variable:}\quad D \equiv D(r) = 1 - \frac{q(r)}{r},\quad D \in [0,1] \tag{11c}$$

$$\text{Internal variable evolution law:}\quad \dot{r},\quad \begin{cases} r \in [r_o, \infty), \\ r_o = r|_{t=0} = \frac{f_t}{\sqrt{E}} \end{cases} \tag{11d}$$

$$\text{Damage criterion in strain space } \mathbb{E}_{\epsilon}\text{:}\quad \bar{F}(\epsilon_{ij}, r) \equiv \tau_{\epsilon} - r \tag{11e}$$

$$\text{Loading-unloading conditions:}\quad \bar{F} \leqslant 0,\ \ \dot{r} \geqslant 0,\ \ \dot{r}\bar{F} = 0,\ \ \dot{r}\dot{\bar{F}} = 0 \tag{11f}$$

$$\text{Softening law :}\quad \dot{q} = H(r)\dot{r},\quad (H = q'(r) \leqslant 0),\quad \begin{cases} q \in [0, r_o], \\ q|_{t=0} = r_o \end{cases} \tag{11g}$$

where r is the strain-like scalar internal variable, q is the stress-like internal variable, H is the hardening-softening modulus, E_{ijkl} is the secant constitutive tensor. The value r_o is the threshold of the initial elastic domain, characterized in terms of the uniaxial elastic strength f_t and the elasticity modulus E.

For the damage criterion (Eq. 11e), this work uses the equivalent strain expression presented by Oliver *et al.* (2006a). This model seems to be suitable for the representation of brittle or quasi-brittle materials, once it allows the degradation occur only in tensile states. An exponential softening law $q(r)$ for the strong discontinuity regime (Eq. 11g) presented in Manzoli *et al.* (2009) was used here.

Regarding the relationship between stress and strain rates, it is given through a constitutive tangent tensor E^t_{ijkl}, which is equal to E_{ijkl} for unloading (or neutral load). Thus:

$$\dot{\sigma}^{\mathcal{S}}_{ij} = E^t_{ijkl}\dot{\epsilon}_{kl} = E_{ijkl}\dot{\epsilon}_{kl} + \dot{E}_{ijkl}\epsilon_{kl}\ ;\ \text{where}\ \ E^t_{ijkl} = E_{ijkl} - \left(\frac{\partial D}{\partial r}\right)\left(\frac{\partial \tau_{\epsilon}}{\partial \epsilon_{kl}}\right)E^o_{ijrs}\epsilon_{rs} \tag{12}$$

The use of CSDA with anisotropic materials is not considered in this work. It would require the adoption of a class of anisotropic damage degradation rule, as described in Simo *et al.* (1993), and in the context of BEM, the adoption of a proper fundamental solution. Nevertheless, it is important to mention there is no necessity to resort to anisotropic continuum model to induce the anisotropic (directional) behavior associated to the discrete constitutive model. This induced discrete model could be considered as directional projections of the continuum, these projections being given by the strong discontinuity kinematics which have a well defined directional term (the normal **n** in Eq. (2)), as mentioned by Oliver (2000).

5. NUMERICAL IMPLEMENTATION FEATURES

The analysis of solids by BEM requires the discretization of its boundary into elements, where the displacements and tractions are approximated. This work considers the use of isoparametric quadrilateral boundary elements, with linear function assumed for the variation of the known (and unknown) boundary values and the boundary shape. For these elements, the regular integrals are performed through standard Gauss quadrature. The accuracy of such integrals is ensured by using the strategy of division into sub-regions when necessary, adapted from the criterion presented by Eberwien *et al.* (2005). On the other hand, for the evaluation of the integrals with weakly singular kernels the element is split in two sub-elements, where a variable transformation allows the integration, as proposed in Lachat and Watson (1976). In contrast, the coefficients with CPV integrals (strongly singular kernels) are evaluated indirectly, using the rigid body motion concept.

The solution of non-linear problems through initial strains approach (ϵ_{ij}^{φ} in the case of cells with embedded discontinuity) requires the discretization of regions of the domain that are likely to present energy dissipation, for the approximation of initial strains. Hexahedral cells with constant function, compatible with uniform displacement jump inside the cell (see Eq. 2), are used in this work, with one functional node placed at the centroid of each cell (collocation point ξ^c). Each cell has the geometry parametrized by conventional linear shape functions (M^{α}), defined by natural coordinates (η_i) and its eight geometrical vertex nodes (α), depicted in Fig. 3.

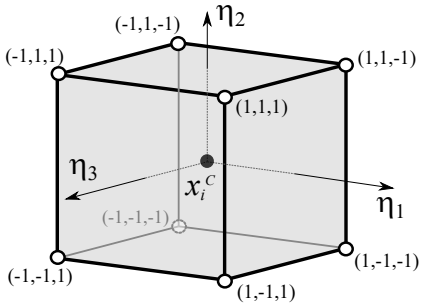

$$x_i(\mathbf{X}) \approx x_i(\eta_1, \eta_2, \eta_3) = \sum_{\alpha=1}^{n} M^{\alpha}(\eta_1, \eta_2, \eta_3) x_i^{\alpha}$$

Figure 3: Hexahedral cell in natural coordinates η_i, geometric nodes ($\circ$) and functional node ($\bullet$).

For each cell, regular integrals are performed with a subdivision strategy similar to that used for boundary elements, while integrals with weakly singular kernels are evaluated through the techniques presented in Lachat and Watson (1976) using sub-cells division (Fig. 4). For the integrals with strongly singular kernels the technique proposed in Gao and Davies (2000) is applied, where the integral can be divided in two parts, in such way that the first part is weakly singular and can be integrated by the technique previously mentioned, whilst the second part, with the strong singularity, is evaluated semi-analytically.

5.1 Cells with embedded discontinuity

As stated in Fig. 1, strong discontinuity dissipative effects are restricted to the sub-domain Ω_{φ}, which needs discretization. For the adopted constant cells, the field ϵ_{ij}^{φ} have only one value inside each cell, *i.e.*, $\epsilon_{ij}^{\varphi} \approx \epsilon^{\varphi,c}$ for $\mathbf{X} \in \Omega_c$. The discontinuity surface inside a cell is, therefore, described by one plane with a unitary vector normal ($\mathbf{n}$) defining its orientation (see Fig. 5). A very small scalar parameter, h is used to regularize the Dirac delta function.

The function $\varphi(\mathbf{X})$ inside a cell can be expressed from the usual geometric parametrization functions (M^{α}), as they are defined by values one or zero at nodes. In this way, the following form is adopted:

$$\varphi(\mathbf{X}(\eta_1, \eta_2, \eta_3)) = \sum_{\varphi^+} M^{\alpha^+}(\eta_1, \eta_2, \eta_3) \tag{13}$$

where the summation is taken over the interpolation functions associated to the geometric vertices located at Ω_c^+ side of

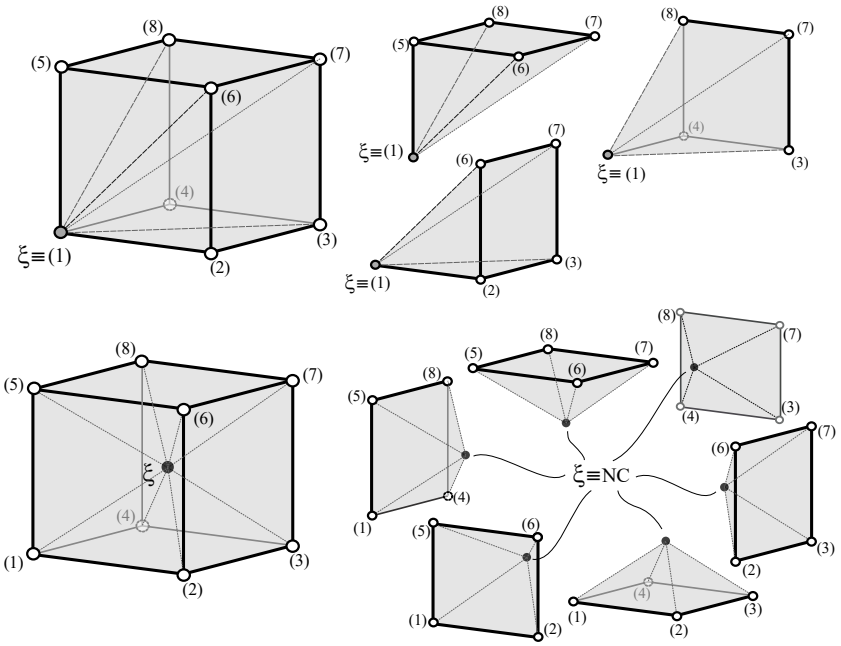

Figure 4: Division of hexahedral constant cell into subcells for integration when the singularity is at a geometric corner node, *e.g.* node 1 (up), or at a functional central node (down).

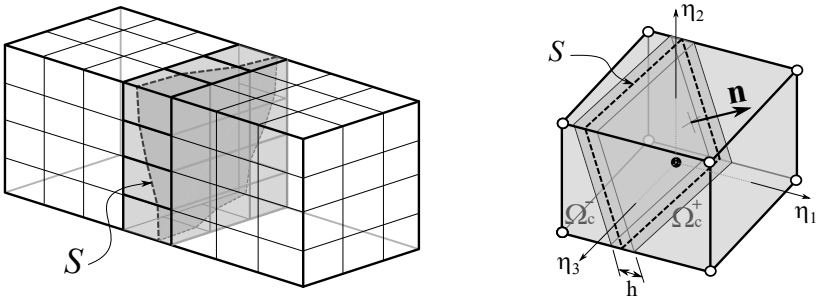

Figure 5: Boundary and domain discretization (left) and a cell with embedded discontinuity (right).

the cell (see Fig. 5).

5.2 Displacement jumps

Inside each cell, the displacement jump components on the discontinuity surface are considered as constants (uniform displacement jumps), *i.e.*, $[\![u_i]\!](\mathbf{X}) \approx [\![u^c]\!]$ for $\mathbf{X} \in \Omega_c$. These values are obtained from the numerical solution of Eq. (3). For this purpose, the inelastic strains at a point inside a cell ($\epsilon^{\varphi,c}$) can be written in terms of the displacement jump as:

$$\begin{Bmatrix} \dot{\epsilon}^{\varphi}_{11}(\mathbf{X}) \\ \dot{\epsilon}^{\varphi}_{22}(\mathbf{X}) \\ \dot{\epsilon}^{\varphi}_{33}(\mathbf{X}) \\ \dot{\epsilon}^{\varphi}_{12}(\mathbf{X}) \\ \dot{\epsilon}^{\varphi}_{13}(\mathbf{X}) \\ \dot{\epsilon}^{\varphi}_{23}(\mathbf{X}) \end{Bmatrix} = \{\epsilon^{\varphi,c}\} = \begin{bmatrix} \varphi_{,1}\left(\boldsymbol{\xi}^c\right) & 0 & 0 \\ 0 & \varphi_{,2}\left(\boldsymbol{\xi}^c\right) & 0 \\ 0 & 0 & \varphi_{,3}\left(\boldsymbol{\xi}^c\right) \\ \frac{1}{2}\varphi_{,2}\left(\boldsymbol{\xi}^c\right) & \frac{1}{2}\varphi_{,1}\left(\boldsymbol{\xi}^c\right) & 0 \\ \frac{1}{2}\varphi_{,3}\left(\boldsymbol{\xi}^c\right) & 0 & \frac{1}{2}\varphi_{,1}\left(\boldsymbol{\xi}^c\right) \\ 0 & \frac{1}{2}\varphi_{,3}\left(\boldsymbol{\xi}^c\right) & \frac{1}{2}\varphi_{,2}\left(\boldsymbol{\xi}^c\right) \end{bmatrix} \begin{Bmatrix} [\![u^c_1]\!] \\ [\![u^c_2]\!] \\ [\![u^c_3]\!] \end{Bmatrix} = [\nabla^s \varphi]\{[\![u^c]\!]\} \tag{14}$$

where $\boldsymbol{\xi}^c$ are the coordinates of the collocation point of cell c and, from Eq. (13),

$$\varphi_{,i} = \frac{\partial \varphi}{\partial \eta_k}\frac{\partial \eta_k}{\partial X_i} = \left(\frac{\partial M^\alpha}{\partial \eta_k} X^\alpha_i\right)^{-1}\left(\frac{\partial}{\partial \eta_k}\left[\sum_{\alpha^+} M^{\alpha^+}\right]\right) \tag{15}$$

Thus, Eq. (3) can be expressed in a matrix form as:

$$\{f\} = [\bar{N}^c]^T\Big([E^o]\{\hat{\epsilon}^c\} - [E^o][\nabla^s\varphi]\{[\![u^c]\!]\} - \{\sigma^{\mathcal{S}}\big(\{\hat{\epsilon}^c\} - [\nabla^s\varphi]\{[\![u^c]\!]\} + \frac{1}{h}[N^c]\{[\![u^c]\!]\}\big)\}\Big) = \{0\} \tag{16}$$

where $[E^o]$ corresponds to the constitutive linear elastic tensor E^o_{ijkl}, the parameter h is a very small scalar used to regularize the Dirac delta function (and, as a consequence, appears in the constitutive model softening law), the vector $\{\sigma^{\mathcal{S}}(\cdot)\}$ corresponds to stress components given by Eq. (11b) with the damage variable taken from Eqs. (11c). Furthermore:

$$[\bar{N}^c]^T = \begin{bmatrix} n_1 & 0 & 0 & n_2 & n_3 & 0 \\ 0 & n_2 & 0 & n_1 & 0 & n_3 \\ 0 & 0 & n_3 & 0 & n_1 & n_2 \end{bmatrix}; \quad [N^c] = \begin{bmatrix} n_1 & 0 & 0 & \frac{1}{2}n_2 & \frac{1}{2}n_3 & 0 \\ 0 & n_2 & 0 & \frac{1}{2}n_1 & 0 & \frac{1}{2}n_3 \\ 0 & 0 & n_3 & 0 & \frac{1}{2}n_1 & \frac{1}{2}n_2 \end{bmatrix}^T \tag{17}$$

For the solution of Eq. (16), given a particular state of regular strain, $\{\hat{\epsilon}^c\}$, the iterative Newton's method is employed, considering that its linearised form is given by:

$$\{f\}_{j-1} + \left[\frac{\partial\{f\}}{\partial\{[\![u^c]\!]\}}\right]_{j-1} \{\delta[\![u^c]\!]\}_j \approx \{0\} \tag{18}$$

where j is an iterative index, $\{\delta[\![u^c]\!]\}_j = \{[\![u^c]\!]\}_j - \{[\![u^c]\!]\}_{j-1}$, and

$$\left[\frac{\partial\{f\}}{\partial\{[\![u^c]\!]\}}\right]_{j-1} = [\bar{N}^c]^T \left[-[E^o][\nabla^s\varphi] - \left[\frac{\partial\sigma^{\mathcal{S}}}{\partial\epsilon}\right]_{j-1} \left[\frac{1}{h}[N^c] - [\nabla^s\varphi]\right]\right] \tag{19}$$

The term $\left[\frac{\partial\sigma^{\mathcal{S}}}{\partial\epsilon}\right]$ is the matrix form of the tangent operator of the continuum constitutive model used to represent the dissipative effects over the discontinuity line $\mathcal{S}$, given in Eq. (12).

5.3 Regularized constitutive model in a cell

The non linear procedure to evaluate the displacement jump, described in the previous section, is performed inside each cell with embedded discontinuity, every iteration during the solution of Eq. (10), in order to update the regularized stress, $\{\tilde{\sigma}\}$, given by Eq. (4). Thus, it is convenient to present here the discrete version of Eq. (4) in a cell, i.e.,

$$\{\tilde{\sigma}(\hat{\epsilon}^c)\} = [E^o](\{\hat{\epsilon}^c\} - \{\epsilon^{\varphi,c}\}) = [E^o](\{\hat{\epsilon}^c\} - [\nabla^s\varphi^c]\{[\![u]\!]\}) \tag{20}$$

Moreover, the tangent operator associated to this regularized constitutive model, is also required for the non linear solution of the equilibrium condition vector, Eq. (10), and can be obtained from differentiation of Eq. (20), expressed in matrix form as:

$$\left[\frac{\partial\tilde{\sigma}}{\partial\hat{\epsilon}^c}\right] = [E^o]\left([I] - [\nabla^s\varphi^c]\left[\frac{\partial\{f\}}{\partial\{[\![u^c]\!]\}}\right]^{-1}[\bar{N}^c]^T\left([E^o] - \left[\frac{\partial\sigma^{\mathcal{S}}}{\partial\epsilon}\right]\right)\right) \tag{21}$$

6. NUMERICAL SIMULATIONS: CUBE UNDER SIMPLE TENSION

This example presents the analysis of a cubic solid under simple traction performed with the presented formulation. Dimensions and material properties are presented in Fig. 6. It is assumed the inception of a failure surface at a plane placed in the center of the solid (between the fixed face and the loaded face), as depicted. Hexahedral cells with embedded uniform strong discontinuity were applied for the discretization of this specific region of the solid. The remaining regions are considered to present elastic behaviour. Initially, even those cells work in elastic regime, until the activation of the strong discontinuity. When such activation occurs, the discontinuity surface plane is oriented perpendicularly to the maximum principal stress direction. Exponential damage evolution was considered for dissipation effects. For the non-linear analyses, the control method adopted to drive the incremental-iterative procedure is the direct displacement, with a convergence tolerance for Eqs. (10) and (16) fixed as 1×10^{-4}. An assumed value of 0.01mm was adopted for the parameter h in Eqs. (16) and (19).

Four different meshes were considered (see Fig. 7), keeping the cubic proportion for the cells, and considering discretization progressively close to the expected discontinuity surface. One of the objectives of this example is to show that the discontinuity is captured in the region of the domain discretized in cells with embedded discontinuities, regardless of the thickness of the discretized region.

Results for the equilibrium path, represented by the cumulative load factor in function of the loaded face displacement, are presented in Fig. 8a, for different meshes. The first mesh considers the whole domain as one cell, while in the fourth mesh only a central strip with 12.5% of the length has the domain discretized. The coincident curves show that the formulation succeeded in eliminating the numerically induced strain localization phenomenon, which is a weakness of discrete modelling when standard continuum constitutive models equipped with softening law.

To illustrate the displacement jump effect, Fig. 8b shows the longitudinal displacement along a lower edge (A-B on Fig. 6) of the solid, for the more refined meshes. The discontinuity in the displacement field at that instant is evidenced,

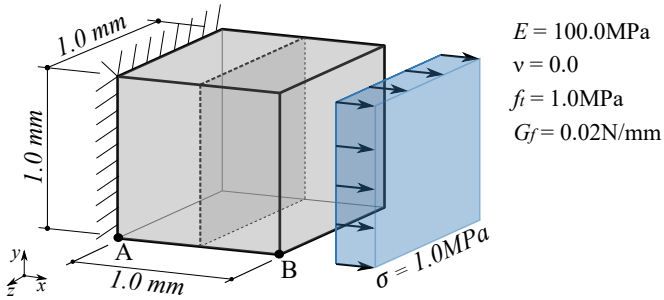

Figure 6: Example 1 - Cubic solid under simple traction with discontinuity surface

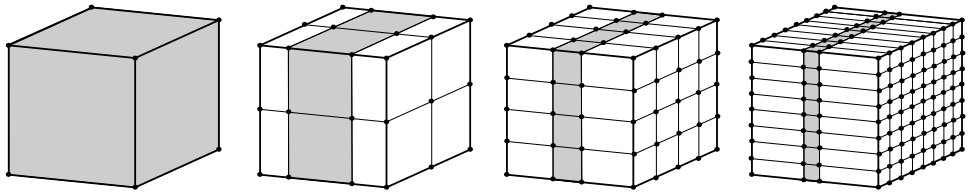

mesh 1 mesh 2 mesh 3 mesh 4

Figure 7: Example 1 - Mesh discretizations - domain in cubic cells

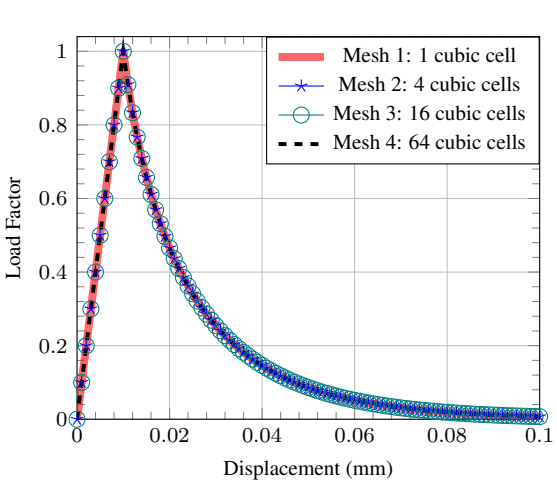

(a) Equilibrium path for displacement at point B

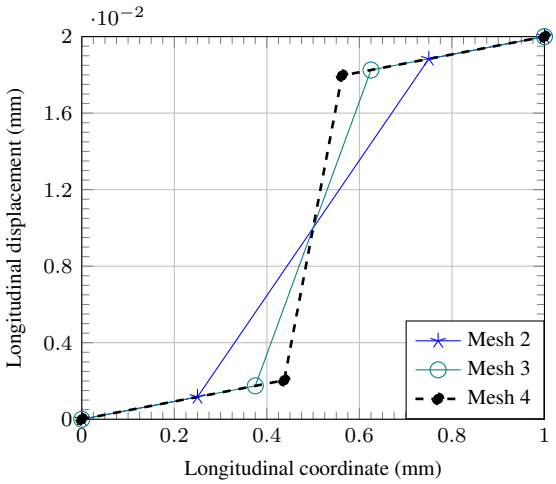

(b) Longitudinal displacement at a lower-edge A-B, for a load-factor = 20% in inelastic regime

Figure 8: Example 1 - Results for meshes with cubic cells

specially for more refined meshes. The refinement of the contour mesh, in the elastic region, does not have significant influence on the results presented. Therefore, results with this kind of refinement are not presented.

In subsequent tests, a different set of non-cubic hexahedral cells were applied for each analysis. The cubic solid (Fig. 6) had the central strip discretized into hexahedral cells with the proportions shown in Fig. 9. The central strip considered had width of 12.5% or 20% of the longitudinal length. Results achieved for the equilibrium path are presented in Fig. 10, where the curve for the use of cubic cells are also plotted as a reference.

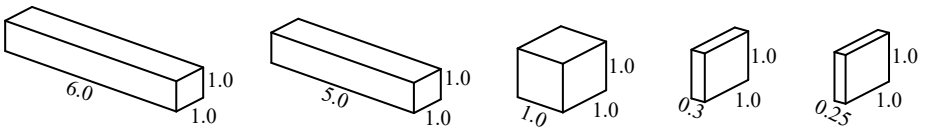

Figure 9: Example 1 - Hexahedral non-cubic cells and its proportions

From these results, one can observe the interference of using cells with very distorted proportion in the results, specially for the inelastic branch of the equilibrium path, which present an incomplete and even meaningless unloading. Similar behaviour was also be observed for two dimensional analysis (plane stress) when quadrilateral cells with high aspect ratio were used. It is worth to mention, however, that the same problem is observed for physically non-linear analysis with standard damage constitutive models, i.e., the lack of a complete stress relief with the damage evolution is

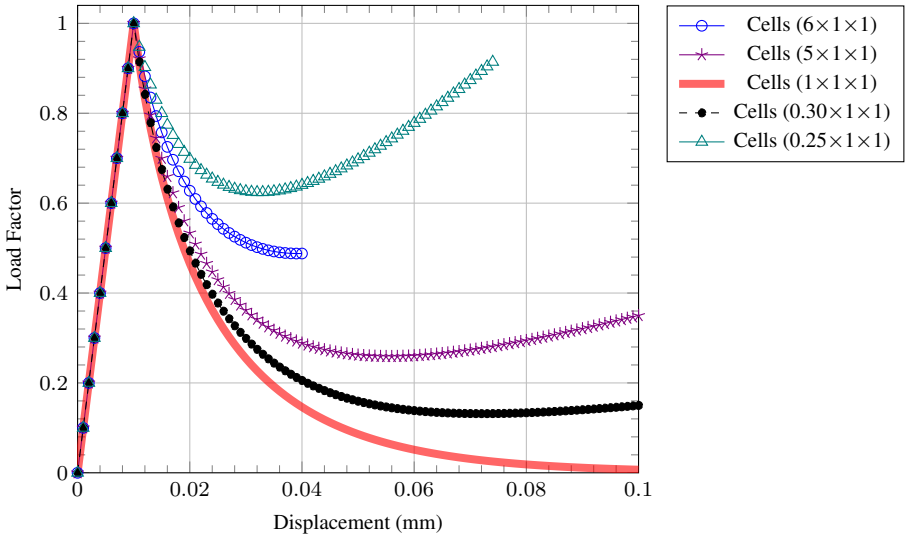

Figure 10: Example 1 - Equilibrium path for displacement at point B for distorted cells with embedded discontinuity

also verified if distorted cells are employed. Moreover, analogous inconsistent results can be observed for cubic cells if integration order is significantly reduced. Thus, the limitation is more related to cells integration loss of accuracy than to the presence of an embedded discontinuity surface, and the use of cells with that distorted proportion do not seems to be suitable.

7. CONCLUSIONS

This work presents some aspects of the use of implicit formulation of the BEM associated with the CSDA and a damage constitutive model for three-dimensional analysis of solids. The results achieved shown a good representation of displacement jumps inside the cells on the discontinuity surfaces. Nevertheless, a strong influence of the use of very distorted cells on results was verified, causing lack of convergence and incomplete or meaningless inelastic unloading. Despite the very simple example presented, the implemented algorithm enables a progressive activation of discontinuity inside the cells, according to the evolution of stress values in the domain. This is an important aspect for the analysis of crack propagation in solids. The potential of the approach allows its sophistication through the implementation of a tracking algorithm for automatic generation of cells in the domain, in order to reproduce a crack propagation. All these stages of evolution has already been successfully developed for bi-dimensional analysis, but are still in course for three-dimensional problems.

8. ACKNOWLEDGEMENTS

The authors gratefully acknowledge the financial support received from the following Brazilian agency of research funding: CNPq - Conselho Nacional de Desenvolvimento Científico e Tecnológico (Grant number 432471/2018-9).

9. REFERENCES

Anacleto, F.E.S., Ribeiro, T.S.A., Ribeiro, G.O., Pitangueira, R.L.S. and Penna, S.S., 2013. "An object-oriented tridimensional self-regular boundary element method implementation". *Engineering Analysis with Boundary Elements*, Vol. 37, pp. 1276–1284.

Benallal, A., Botta, A.S. and Venturini, W.S., 2006. "On the description of localization and failure phenomena by the boundary element method". *Computer Methods in Applied Mechanics and Engineering*, Vol. 195, pp. 5833–5856.

Botta, A.S., Venturini, W.S. and Benallal, A., 2005. "BEM applied to damage models emphasizing localization and associated regularization techniques". *Engineering Analysis with Boundary Elements*, Vol. 29, pp. 814–827.

Eberwien, U., Duenser, C. and Moser, W., 2005. "Efficient calculation of internal results in 2d elasticity bem". *Engineering Analysis with Boundary Elements*, Vol. 29, pp. 447–453.

Gao, X.W. and Davies, T.G., 2000. "An effective boundary element algorithm for 2D and 3D elastoplastic problems". *International Journal of Solids and Structures*, Vol. 37, pp. 4987–5008.

Lachat, J.C. and Watson, J.O., 1976. "Effective numerical treatment of boundary integral equations – A formulation for three dimensional elastostatics". *International Journal for Numerical Methods in Engineering*, Vol. 10, pp. 991–1005.

Lin, F.B., Yan, G., Bazant, Z.P. and Ding, F., 2002. "Non-local strain-softening model of quasi-brittle materials using boundary element method". *Engineering Analysis with Boundary Elements*, Vol. 26, pp. 417–424.

Manzoli, O.L., Pedrini, R.A. and Venturini, W.S., 2009. "Strong discontinuity analysis in solid mechanics using boundary element method". In E.J. Sapountzakis and M.H. Aliabadi, eds., *Advances in Boundary Element Techniques X - Proceedings of the 10th International Conference (BETEQ 2009)*. Athens, Greece, pp. 323–329.

Manzoli, O.L. and Venturini, W.S., 2004. "Uma formulação do MEC para simulação numérica de descontinuidades fortes". *Revista Internacional de Métodos Numéricos para Cálculo y Diseño en Ingeniería*, Vol. 20, No. 3, pp. 215–234.

Manzoli, O.L. and Venturini, W.S., 2007. "An implicit BEM formulation to model strong discontinuities". *Computational Mechanics*, Vol. 40, pp. 901–909.

Mariani, S. and Perego, U., 2003. "Extended finite element method for quasi-brittle fracture". *International Journal for Numerical Methods in Engineering*, Vol. 58, pp. 103–126.

Mendonça, T.S., Peixoto, R.G. and Ribeiro, G.O., 2020. "A new class of cells with embedded discontinuity for fracture analysis by the boundary element method". *International Journal for Numerical Methods in Engineering*, Vol. 121, pp. 3869–3892.

Oliver, J., 2000. "On the discrete constitutive models induced by strong discontinuity kinematics and continuum constitutive equations". *International Journal of Solids and Structures*, Vol. 37, pp. 7207–7229.

Oliver, J., Cervera, M. and Manzoli, O., 1998. "On the use of strain-softening models for the simulation of strong discontinuities in solids". In R. de Borst and E. van der Giessen, eds., *Material instabilities in solids*, John Wiley & Sons, Chichester, chapter 8, pp. 107–123.

Oliver, J., Cervera, M. and Manzoli, O., 1999. "Strong discontinuities and continuum plasticity models: the strong discontinuity approach". *International Journal of Plasticity*, Vol. 15, pp. 319–351.

Oliver, J., Huespe, A.E., Blanco, S. and Linero, D.L., 2006a. "Stability and robustness issues in numerical modeling of material failure with the strong discontinuity approach". *Computer Methods in Applied Mechanics and Engineering*, Vol. 195, pp. 7093–7114.

Oliver, J., Huespe, A.E., Pulido, M.D.G. and Chaves, E., 2002. "From continuum mechanics to fracture mechanics: the strong discontinuity approach". *Engineering Fracture Mechanics*, Vol. 69, pp. 113–136.

Oliver, J., Huespe, A.E. and Samaniego, E., 2003. "A study on finite elements for capturing strong discontinuities". *International Journal for Numerical Methods in Engineering*, Vol. 56, pp. 2135–2161.

Oliver, J., Huespe, A.E. and Sánchez, P.J., 2006b. "A comparative study on finite elements for capturing strong discontinuities: E-FEM vs X-FEM". *Computer Methods in Applied Mechanics and Engineering*, Vol. 195, pp. 4732–4752.

Peixoto, R.G., Anacleto, F.E.S., Ribeiro, G.O., Pitangueira, R.L.S. and Penna, S.S., 2016. "A solution strategy for non-linear implicit BEM formulation using a unified constitutive medelling framework". *Engineering Analysis with Boundary Elements*, Vol. 64, pp. 295–310.

Peixoto, R.G., Ribeiro, G.O. and Pitangueira, R.L.S., 2018. "A boundary element method formulation for quasi-brittle material fracture analysis using the continuum strong discontinuity approach". *Engineering Fracture Mechanics*, Vol. 202, pp. 47–74.

Peixoto, R.G., Ribeiro, G.O., Pitangueira, R.L.S. and Penna, S.S., 2017. "The strong discontinuity approach as a limit case of strain localization in the implicit bem formulation". *Engineering Analysis with Boundary Elements*, Vol. 80, pp. 127–141.

Simo, J.C., Oliver, J. and Armero, F., 1993. "An analysis of strong discontinuities induced by strain-softening in rate-independent inelastic solids". *Computational Mechanics*, Vol. 12, pp. 277–296.

Sládek, J., Sládek, V. and Bazant, Z.P., 2003. "Non-local boundary integral formulation for softening damage". *International Journal for Numerical Methods in Engineering*, Vol. 57, pp. 103–116.

Telles, J.C.F. and Brebbia, C.A., 1979. "On the application of the boundary element method to plasticity". *Applied Mathematical Modelling*, Vol. 3, No. 4, pp. 466–470.

Telles, J.C.F. and Carrer, J.A.M., 1991. "Implicit procedures for the solution of elastoplastic problems by the boundary element method". *Mathematical and Computer Modelling*, Vol. 15, pp. 303–311.

10. RESPONSIBILITY NOTICE

The authors are solely responsible for the printed material included in this paper.